Changes in Drought Characteristics over China Using the Standardized Precipitation Evapotranspiration Index

HUOPO CHEN

Nansen-Zhu International Research Centre, Institute of Atmospheric Physics, Chinese Academy of Sciences, and University of Chinese Academy of Sciences, Beijing, and Collaborative Innovation Center on Forecast and Evaluation of Meteorological Disasters, Nanjing University of Information Science and Technology, Nanjing, China

JIANQI SUN

Nansen-Zhu International Research Centre, Institute of Atmospheric Physics, Chinese Academy of Sciences, and University of Chinese Academy of Sciences, Beijing, China

(Manuscript received 16 October 2014, in final form 8 March 2015)

ABSTRACT

The standardized precipitation evapotranspiration index (SPEI) is computed and compared in China using reference evapotranspiration calculated using the Thornthwaite (TH) approach and the Penman–Monteith (PM) equation. The analysis reveals that SPEI_PM outperforms the SPEI_TH with regard to drought monitoring during the period 1961–2012 over China, especially in arid regions of China. Furthermore, the SPEI_PM also performs better with regard to observed variations in soil moisture and streamflow in China. Thus, changes in drought characteristics over China are detected on the basis of variations in the SPEI_PM. The results indicate that droughts over China exhibit pronounced decadal variations over the past 50 yr, with more frequent and severe droughts occurring before the 1980s and in the 2000s compared with the 1980s and 1990s. Since the late 1990s, droughts have become more frequent and severe across China, especially in some regions of northern China. Concurrently, consecutive drought events have also increased across China. This suggests that dry conditions in China have been enhanced in recent years. Further analyses illustrate that the temperature and precipitation anomalies exhibit different roles in detecting droughts across China, which is primarily due to the magnitude of their variations and different climate variability. Considering temperature and precipitation perturbations, droughts exhibit relatively larger responses to temperature fluctuations in northern China and relatively larger responses to precipitation anomalies in southern China.

1. Introduction

Drought is a major natural hazard that is characterized by below-average precipitation over a long period of time. Droughts are recognized as one of the main natural causes of agricultural, economic, and environmental damages. Moreover, droughts occur over most parts of the world, even in humid regions. A large drying trend can be observed over many land areas since the mid-1950s, with widespread drying over much of northern Africa, Alaska, Canada, and Eurasia (Dai et al. 2004; Dai 2012; Spinoni et al. 2014). Previous work has suggested that dry areas increased by approximately 1.74% decade^{-1} from 1950 to 2008 (Dai 2011a). Many studies have attributed most of this drying to the recent global warming (e.g., Field et al. 2012). The Fifth Assessment Report (AR5) of the Intergovernmental Panel on Climate Change (IPCC) indicated that continued emissions of greenhouse gases would definitely cause additional warming (Stocker et al. 2013), enhancing dry conditions in the future. Thus, a rising concern regarding this issue is common both within government bodies and among the general public.

Because of the impacts of large-scale climate variability, including the East Asian monsoon, China has suffered from several prolonging severe drought disasters that have had major effects on some sectors, such as agriculture, industry, society, and ecosystems

Corresponding author address: Huopo Chen, Nansen-Zhu International Research Centre, Institute of Atmospheric Physics, Chinese Academy of Sciences, P.O. Box 9804, Beijing 100029, China.
E-mail: chenhuopo@mail.iap.ac.cn

DOI: 10.1175/JCLI-D-14-00707.1

(Song et al. 2003; Zou et al. 2005; Ma and Fu 2006; Xin et al. 2006; Lu et al. 2011; Wang et al. 2011; Yan et al. 2011; Wang et al. 2012; Liu and Jiang 2014). Based on historical records, Zou et al. (2005) indicated that drought areas in north China have significantly increase based on the Palmer drought severity index (PDSI). Yu et al. (2014) also revealed that severe and extreme droughts have become more serious since the late 1990s in China, and the dry areas were reported to increase by ~3.72% decade^{-1} in the past five decades. In any particular year, there is typically a region in China that endures a precipitation deficit and experiences drought, leading to large societal and economic losses. The severe drought in 1997 over northern China caused continuous zero flow in the Yellow River for nearly 226 days (Cong et al. 2009). Drought has also occurred in the Yangtze River basin, with runoff reaching a 50-yr low in 2006 (Yu et al. 2013). Both the long-term drought from autumn 2009 to spring 2010 across southwest China and the short-term drought in July–August 2013 over the Jiangnan region (with air temperatures up to 42.7°C in Zhejiang Province) resulted in drinking water shortages for people and livestock and nearly no crop harvest (Huang et al. 2012; Yang et al. 2012; Duan et al. 2013; Sun 2014). Such severe droughts have been documented throughout the instrumental records and are certain to continue in the future (Chen et al. 2013; Wang et al. 2014).

Because of the complexity of drought variability, it is challenging to objectively quantify drought intensity, duration, and spatial extent (Dai 2011a). Thus, numerous studies have attempted to improve drought detection and monitoring; a few objective indices have been developed on the basis of readily available data, such as precipitation and temperature (e.g., Palmer 1965; McKee et al. 1993; Ma and Fu 2001). Among these indices, the PDSI, which is based on supply and demand in the water balance, is one of the most widely used drought indices in the world. However, the PDSI has several deficiencies, including the strong influence of the calibration period, the limitation in spatial comparability, and subjectivity in relating drought conditions to the index values. Many of these problems were resolved with the development of the self-calibrated PDSI (Wells et al. 2004); however, the main shortcoming, that is, the built-in fixed time scale (9–12 months), has not been resolved (Guttman 1998). Based on the multiscale characteristics of droughts, the standardized precipitation index (SPI), which is based on a probabilistic precipitation approach, has been developed (McKee et al. 1993) and widely accepted in both research and operational work in recent years (e.g., Gao and Yang 2009; Chen et al. 2013; Orlowsky and Seneviratne 2013). However, only the precipitation variability is considered in the SPI calculation; the role of temperature is ignored. The effect of temperature is evident in initiating droughts, although droughts are primarily caused by below-average precipitation. Nevertheless, results from global climate model simulations have indicated that drought induced by warming is well predicted using the PDSI, while no excepted changes are indicated using the SPI (Dubrovsky et al. 2009). Therefore, a new standardized precipitation evapotranspiration index (SPEI) was developed by Vicente-Serrano et al. (2010) and further improved by Beguería et al. (2014). This index is also based on the supply and demand concept of the water balance equation. Thus, the SPEI not only considers the effects of temperature on drought severity but also considers the multiscale characteristics that are incorporated in the SPI. Thus far, our understanding of global and regional drought conditions has been primarily derived from variations in these drought indices.

The calculation of the SPEI is as simple as computing the SPI; however, the water balance is represented by the difference between precipitation and evapotranspiration ($P - E$) rather than only precipitation. Generally, the reference evapotranspiration (ET) is calculated from temperature data using the empirical Thornthwaite equation (TH; Thornthwaite 1948). However, many previous studies have indicated that ET is underestimated in arid and semiarid regions (Jensen et al. 1990) and overestimated in humid regions (van der Schrier et al. 2011) using this approach because ET is not solely determined by the ambient temperature. ET calculations should include correct physics that account for radiative and aerodynamic impacts (Roderick et al. 2007). Thus, the Food and Agriculture Organization of the United Nations (FAO) Penman–Monteith (PM) method, which is a more realistic calculation that accounts for changes in available energy, humidity, and wind speed, is recommended for computing ET (Allen et al. 1998). Furthermore, a few recent studies have claimed that the drought indices provide better estimates of the true global drought trend when using the PM evapotranspiration framework because of its more comprehensive physics (Sheffield et al. 2012; Trenberth et al. 2014). Hence, the FAO PM method will be included in the SPEI calculations. Moreover, a discussion of the aridity changes in China using updated data from 1960 to 2012 will be provided in this study, further improving our understanding of warming-induced drought changes in China.

2. Data and methods

a. Data

First, the SPEI is determined using two different reference evapotranspiration calculations, that is, the

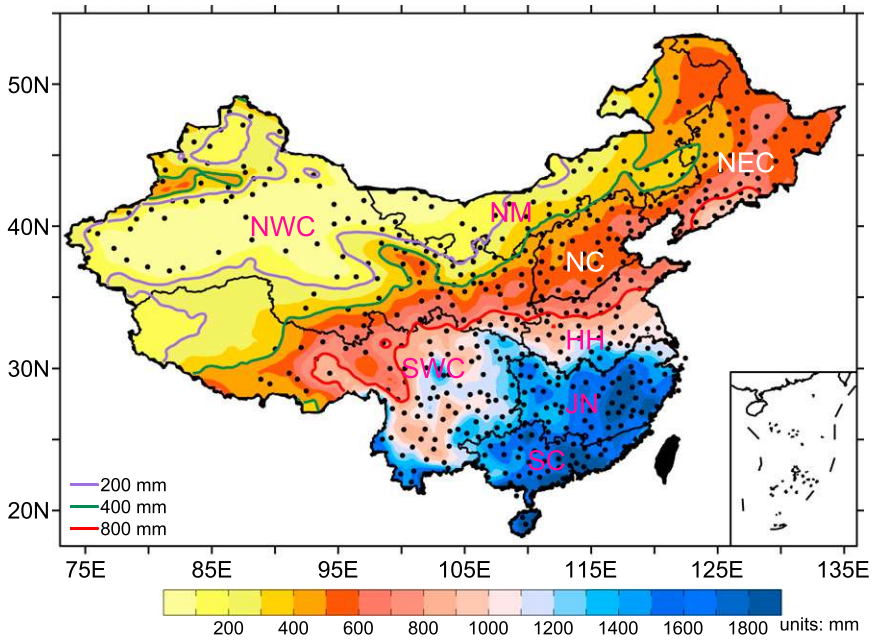

FIG. 1. Locations of the 564 meteorological stations in China and the associated eight subregions (NEC, NC, HH, JN, SC, SWC, NWC, and NM); the arid, semiarid, semihumid, and humid regions are also depicted.

empirical Thornthwaite equation (SPEI_TH) and the more sophisticated Penman–Monteith method (SPEI_PM). The PM equation requires extensive amounts of data, including solar radiation, temperature, wind speed, and relative humidity. These monthly datasets (in addition to precipitation data) are collected for the period 1951–2012 from the National Meteorological Information Center of the China Meteorological Administration (CMA) based on observations from 756 meteorological stations. The homogeneity and reliability of these monthly meteorological datasets have been checked and firmly quality controlled before being release. Although these datasets have been available since 1951, there are many missing data in the 1950s over most of China. Thus, the target period in this study is from 1960 to 2012. Based on the data for these 53 yr, if a given site is missing 5% of the time series, the site is rejected. Accordingly, a subset of 564 stations is selected and there are 80 sites that still have missing records. These missing monthly records are replaced by the climatological values for the period 1960–2012. The locations of these meteorological stations are shown in Fig. 1.

Three additional monthly datasets are also used in this study to compare with the SPEI_TH and SPEI_PM trends, including site-observed soil moisture, streamflow, and the self-calibrated PDSI. First, the monthly soil moisture ($m^3 m^{-3}$) data are collected from CMA based on observations at 226 meteorological stations in China; the dataset consists of information for the top 10-, 20-, and 50-cm layers and encompasses the period 1993–2008. Second, the observed monthly streamflow data during the period 1962–2000 from Harbin station, which is located in the Songhua River basin of northeastern China, are used. Third, the PDSI data used in this study are the monthly self-calibrated PDSI values using the more sophisticated PM equation to estimate the potential evapotranspiration (scPDSI_PM); the PDSI data are based on historical data (Dai 2011b), which have been updated for the period 1850–2012.

Because of the large area of China, the Chinese climate is very complex and varies substantially from region to region. According to annual precipitation data, China can be divided into four climatic regions: arid, semiarid, semihumid, and humid regions (Fig. 1). The arid climate dominates most of northwestern China, with annual precipitation amounts of less than 200 mm. The semiarid and semihumid regions exhibit annual precipitation amounts ranging from 200 to 400 mm and from 400 to 800 mm, respectively. The climate in the humid region, which is primarily confined to southern China, is much wetter, with annual precipitation amounts exceeding 800 mm (Zheng et al. 2013). Climate changes are generally different among these regions; therefore, drought variabilities are discussed in this study. Among the 564 stations, there are 66 stations in

the arid region, 70 in the semiarid region, 177 in the semihumid region, and 251 in the humid region, respectively. Additionally, China is divided into eight subregions, including northeast China (NEC), north China (NC), Huang-Huai basin (HH), Jiangnan (JN), south China (SC), southwest China (SWC), northwest China (NWC), and Neimeng (NM); these regions are used in the following discussion. These divisions are based on the China meteorological and geographical division handbook that was released by the National Meteorological Center of the CMA in 2006; this information can also be found in other studies (e.g., Chen et al. 2012a).

b. Calculation of ET

Two methods are used to calculate ET in this study.

First, the simple Thornthwaite approach (Thornthwaite 1948) is used to calculate ET, which is advantageous because the method only requires monthly temperature data:

$$\mathrm{ET} = 16K\left(\frac{10T_{\mathrm{mm}}}{I}\right)^{m}, \tag{1}$$

where T_{mm} is the monthly mean temperature (°C); I is the heat index, which is calculated from the monthly temperature; m is a coefficient depending on I; and K is a correction coefficient that is computed as a function of the latitude and month.

ET is also computed using the sophisticated Penman–Monteith method (Allen et al. 1998), which is based on underlying physical principles and accounts for both thermodynamic and aerodynamic effects:

$$\mathrm{ET} = \frac{0.408\Delta(\mathrm{Rn} - G) + \gamma[900/(T + 273)]U_2(e_s - e_a)}{\Delta + \gamma(1 + 0.34U_2)}, \tag{2}$$

where Δ is the slope of the saturation vapor pressure curve (kPa °C^{-1}); Rn is the net radiation (MJ m^{-2} day^{-1}); G is the soil heat flux density, which is considered to be 0 for daily estimates; T is the daily mean air temperature (°C) at a height of 2 m, which is based on the average of the observed maximum and minimum temperatures; U_2 is the averaged wind speed at a height of 2 m (m s^{-1}); e_s is the saturation vapor pressure (kPa); e_a is the ambient vapor pressure (kPa); $(e_s - e_a)$ is the saturation vapor pressure deficit at temperature T; and γ is the psychrometric constant (0.0677 kPa °C^{-1}).

Solar radiation data are not available from the meteorological stations in China; therefore, an empirical formulation recommended by Allen et al. (1998) is used here to calculate the net radiation based on the observed number of sunshine hours. The saturation vapor pressure deficit is determined based on the relative humidity and the maximum and minimum temperatures. Additionally, assuming a logarithmic wind speed profile, the observed wind speed at a height of 10 m is converted to the standard height of 2 m for use in the aforementioned calculation. For more approximations and details please refer to Sentelhas et al. (2010).

TABLE 1. Categorization of dry and wet grade according to the SPEI and the corresponding cumulative probability relative to the base period.

Categorization	SPEI	Cumulative probability
Extremely dry	Less than −2	0.0228
Severe dry	−1.99 to −1.5	0.0668
Moderate dry	−1.49 to −1.0	0.1587
Normal	−1.0 to 1.0	0.5000
Moderate wet	1.0 to 1.49	0.8413
Severe wet	1.5 to 1.99	0.9332
Extremely wet	Larger than 2	0.9772

Before calculating the SPEI, the differences in Penman–Monteith and Thornthwaite evapotranspiration are analyzed (figure not shown). Results indicate that the ET_PM is relatively greater, by 20% or more, over most regions of northern China and southwest China than ET_TH. However, over most regions of southern China and northeast China, the ET_PM is relatively less than ET_TH. These results agree well with early studies (Jensen et al. 1990; van der Schrier et al. 2011).

Then, the SPEI_TH and SPEI_PM are calculated at different time scales for each station based on the accumulated deficit and surplus, that is, the climate water balance $(P - E)$. This computation is the same procedure used to determine the SPI; more information can be found in Vicente-Serrano et al. (2010). Table 1 shows the categorization of the dryness–wetness grade according to the SPEI and the corresponding cumulative probability in relation to the base period.

c. Analysis methods

The greatest advantage of the SPEI is its representation of multiple time scales, which allows the monitoring of different drought types, such as meteorological, agricultural, hydrological, and societal drought. In this study, the drought characteristics represented by the SPEI with 3- and 12-month scales are primarily investigated, including the area, frequency, and intensity. Before calculating the drought area, the site-specific SPEI is resampled to 0.5° × 0.5° grids (longitude by latitude) using the inverse distance-weighting interpolation method. Then, the drought area is computed

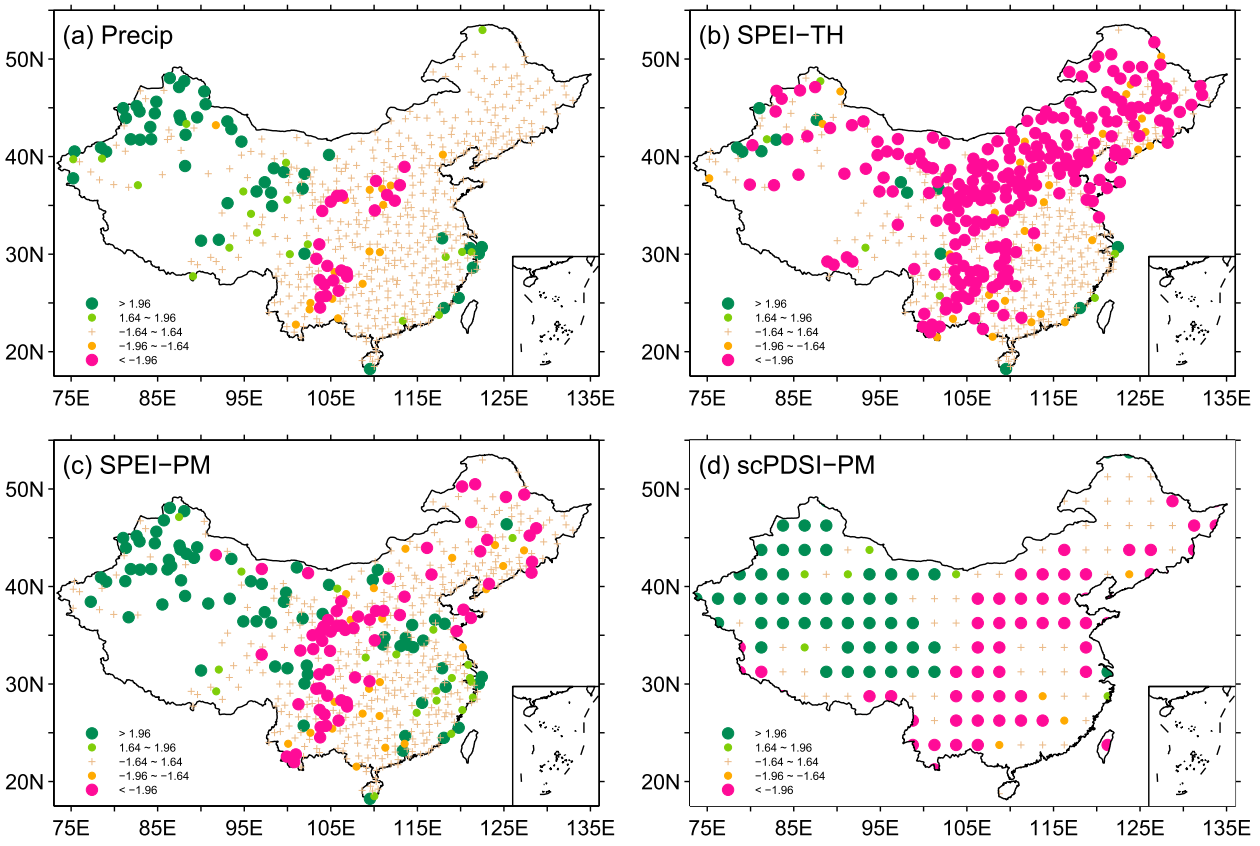

FIG. 2. Spatial distributions of the MK trend statistic for the (a) annual precipitation, (b) annual SPEI_TH (12 months), (c) annual SPEI_PM (12 months), and (d) annual scPDSI_PM based on the period 1961–2012. The significance levels of 5% and 10% are shown.

as the sum of the weighted (cosine function of latitude) grid area for the SPEI < -1.0. The drought frequency is simply defined as the number of months in which the SPEI < -1.0; the corresponding mean SPEI value is the intensity. Additionally, the variations in consecutive dry events (at least 6 months) are also investigated. To analyze the drought characteristic variations in China, Sen's slop method (Sen 1968) is used in this study to calculate the linear trend; the nonparametric Mann–Kendall (MK) approach is applied for its significance test.

3. Comparison of the SPEI_PM to SPEI_TH for monitoring drought in China

Previous studies have documented that there is nearly no difference between the SPEI_PM and SPEI_TH for monitoring drought in some regions, especially from a global perspective (e.g., Beguería et al. 2014). Is this true in China? This question has not been answered; therefore, the focus of this study is to address this question.

Figure 2 shows the spatial patterns of the MK trend statistics for the annual precipitation, SPEI_TH, SPEI_PM, and scPDSI_PM in China for the period 1961–2012. The positive and negative values represent trends toward wetter and drier conditions, respectively. Based on Fig. 2a, the annual precipitation changes in China exhibit large, regional differences over the past 50 yr, with significant upward (wetting) trends over NWC, eastern Tibet, and the coastlines of JN and SC and significant downward (drying) trends over western NC and eastern SWC. Here, a significant trend means that it passed the MK test at the 5% and 10% significance levels. The wetting trend in NWC is consistent with the recent study by Chen et al. (2012b), who indicated that NWC has experienced a remarkable wet shift since the mid-1980s.

Similarly, Fig. 2b presents the variations in the spatial patterns of the annual SPEI_TH. Significant drying trends are found for most regions in China; significant wetting trends are detected over only a few stations in Xinjiang, coastal eastern China, and SWC. The variations in the annual SPEI_PM exhibit much larger differences than the SPEI_TH, especially over NWC (Fig. 2c). Similar to the annual precipitation changes, the annual SPEI_PM exhibits significant trends toward wetter conditions over most stations in NWC. Although

there are no pronounced annual precipitation changes over NEC, NM, and eastern NC, the variations in both the annual SPEI_TH and SPEI_PM consistently exhibit drying trends over the past 50 yr. However, more stations experiencing significant drying trends at the 95% confidence level are found in the SPEI_TH than in the SPEI_PM. The drying conditions over western NC, eastern NWC, and eastern SWC are well captured by both the SPEI_TH and the SPEI_PM, although more stations exhibit significant trends according to the SPEI_TH. Significant trends toward wetter conditions are detected over some small areas in JN and SC according to the SPEI_TH, while larger areas are reported using the SPEI_PM. The annual SPEI_TH changes exhibit no obvious trends in HH, while significant wetting trends are detected by the SPEI_PM. The SPEI_PM changes in this region are much more realistic than that of the SPEI_TH because the rain belt has been observed to experience a northward shift since 2000 (Si et al. 2009; Zhu et al. 2011).

To further validate the performance of the SPEI_TH and the SPEI_PM, the spatial distribution of the MK trend statistic for the annual scPDSI_PM is also presented for China (Fig. 2d). Clearly, significant trends toward wetter conditions are also detected over western China and some coastal areas of eastern China; significant downward trends are found in the other regions. This spatial pattern of scPDSI_PM changes is similar to that of the annual precipitation and the SPEI_PM, while there are some discrepancies with the SPEI_TH in some regions, especially over western China.

Based on the above analysis, we can conclude that the effect of temperature changes is amplified in the SPEI_TH with regard to monitoring drought over China. Particularly over NWC, where the annual precipitation is less than 200 mm, the drying trends in the annual SPEI_TH are primarily attributed temperature increases. Thus, the wet shift in the mid-1980s cannot be captured by the SPEI_TH. When the more realistic reference evapotranspiration calculation is used, the role of temperature changes is restrained because wind speeds and vapor pressure deficits are also considered. This is especially true in the arid regions of China. However, only a slight difference between SPEI_TH and SPEI_PM is found in the humid regions because there is enough precipitation in this region for evapotranspiration to occur and nearly no difference in the variations of $P - E$ (figure not shown).

The changes in the annual SPEI_TH and SPEI_PM are also compared with soil moisture variations in different layers. Figure 3a presents the spatial distribution of the site-observed soil moisture (top 10-cm layer) over China for the period 1993–2008. Significant wetting trends can be seen over most of NWC, NC, HH, and Tibet, while significant drying trends are well defined over some areas of NEC and NM. The SPEI_TH (Fig. 3b) and the SPEI_PM (Fig. 3c) both depict significant drying trends for most stations over NWC, although the SPEI_PM captures wetting trends for some stations in this region. Additionally, the wetting trends over some stations in NC, HH, and southern NEC represented in the soil moisture data are well monitored by the SPEI_PM but not by the SPEI_TH. Similar results can be obtained based on soil moisture changes in the other two studied layers.

The SPEI_PM also performs better at monitoring streamflow variations than the SPEI_TH. Despite the high correlations between the streamflow and the two SPEIs (0.56 for the SPEI_TH and 0.59 for the SPEI_PM, respectively), the increasing trend in the streamflow is only captured by the SPEI_PM; the SPEI_TH exhibits a decreasing trend. However, there are some uncertainties regarding this result due to data limitations; more materials are needed for further verification in the future.

Briefly, the SPEI_PM is much better for monitoring drought over China than the SPEI_TH, particularly over the arid regions. Therefore, the changes in drought characteristics over China during the past 50 yr are investigated in the following section using the SPEI_PM.

4. Drought changes over China

Figure 4 presents the temporal variations in the drought area in China during the period 1961–2012. The drought area in China exhibits a well-defined interdecadal shift according to the SPEI_PM, with a relatively large dry area before the 1980s and from the late 1990s to the present, and a relatively small dry area from the mid-1980s into the 1990s. Based on a comparison of the drought areas during the two dry periods, we find that the current dry conditions in China are not as intense as the earlier period; moreover, the strongest dry conditions occurred primarily in the 1960s. Similar variations in drought area are observed in different levels of drought severity.

The temporal variations in drought area over arid, semiarid, semihumid, and humid regions in China are shown in Fig. 5. Similar characteristics in the drought area variations are found for these four regions, that is, a relatively large dry area was present in the 1960s, 1970s, early 1980s, and since the late 1990s, while a relatively small dry area was present from the mid-1980s into the 1990s. However, there are some well-defined differences among these regions. For the arid region, vast drought events occurred primarily in the 1960s and the 1970s. Despite an increase in drought area in the 2000s

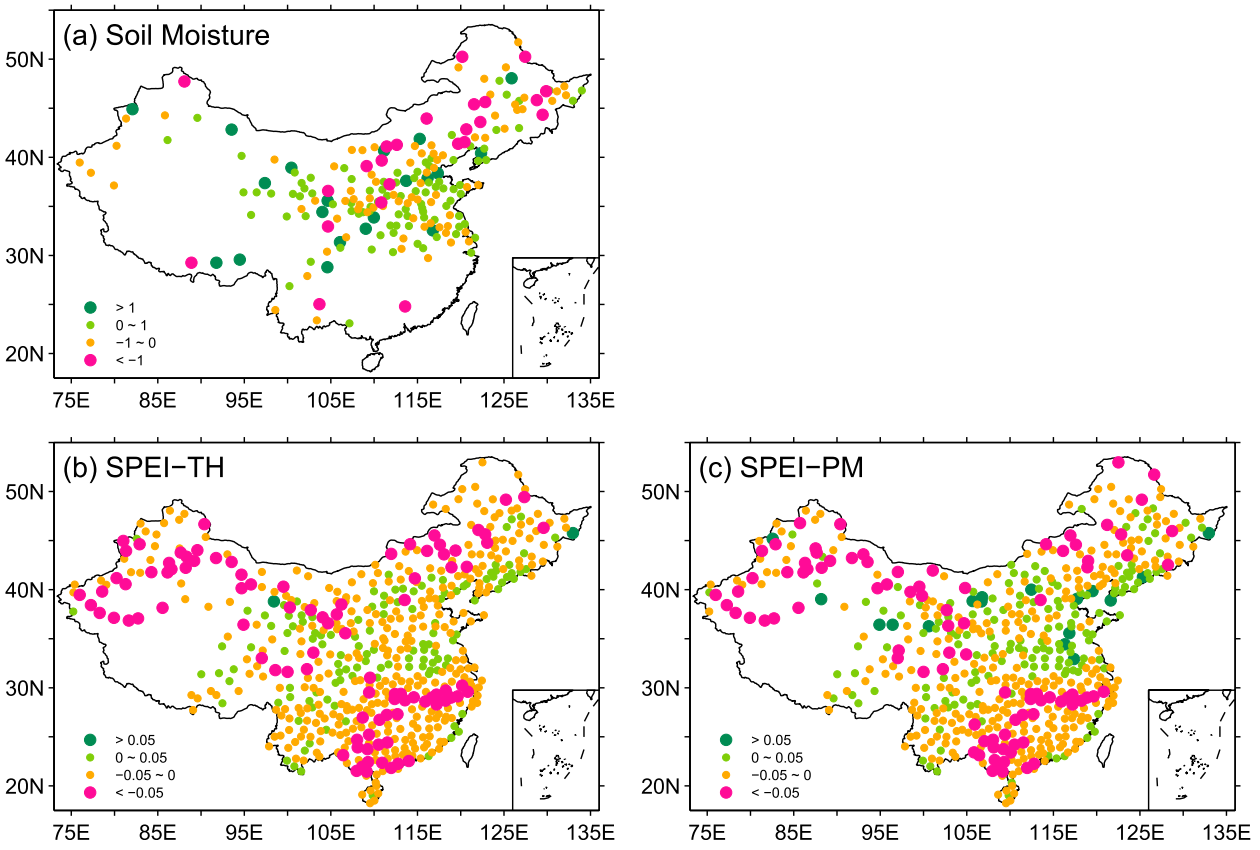

FIG. 3. Trend variations in the (a) annual soil moisture in the top 10-cm layer, (b) annual SPEI_TH (3 months), and (c) annual SPEI_PM (3 months) for the period 1993–2008.

compared to the 1990s, the current drought area remains much smaller than that in the 1960s and the 1970s. Drought area changes in the semiarid region are similar to that of the arid region, while relatively large differences are found when comparing both the semihumid and humid regions to the arid and semiarid regions. For the semihumid region, the drought area increased significantly beginning in the late 1990s, and the variations in drought area are comparable to the 1960s and 1970s. Furthermore, extensive droughts have occurred more frequently since the late 1990s when compared to earlier periods in this region. The drought area in the humid region has also exhibited significant increases since the late 1990s; the drought that occurred from winter 2011 to spring 2012 across southwest China, including Yunnan, Guangxi, Guizhou, Sichuan, and Chongqing Provinces, was the largest drought over the previous 50-yr period. Nevertheless, the frequency of droughts has increased. Briefly, drought areas have dramatically increased since the late 1990s in both the humid and semihumid regions, while smaller changes are detected in the arid and semiarid regions.

Based on the above analysis, a significant decadal change in drought area has occurred during recent decades in both China and its associated subregions. To better understand the dry conditions in China, the characteristics of the decadal changes in drought events are investigated for two dry periods (i.e., 1970–80 and 2000–10) and a wet period (i.e., 1985–95). Figure 6 shows the spatial patterns of the decadal changes in drought frequency, which are represented by the monthly number of occurrences in which the SPEI < -1.0 in China. In the period 1985–95, the drought frequency decreased over most of China when compared to the earlier period, especially in northern China, including stations in NWC, NC, NM, and NEC. A decrease also occurred for most stations in eastern Tibet. However, several sparse stations in SC and eastern SWC have suffered from increasing drought frequency. These changes reversed in the early portion of the current century; the drought frequency began to increase over most areas of China. In NC and NEC, the drought frequency increased substantially for a few stations during the period 2000–10 relative to the period 1985–95; however, drought events

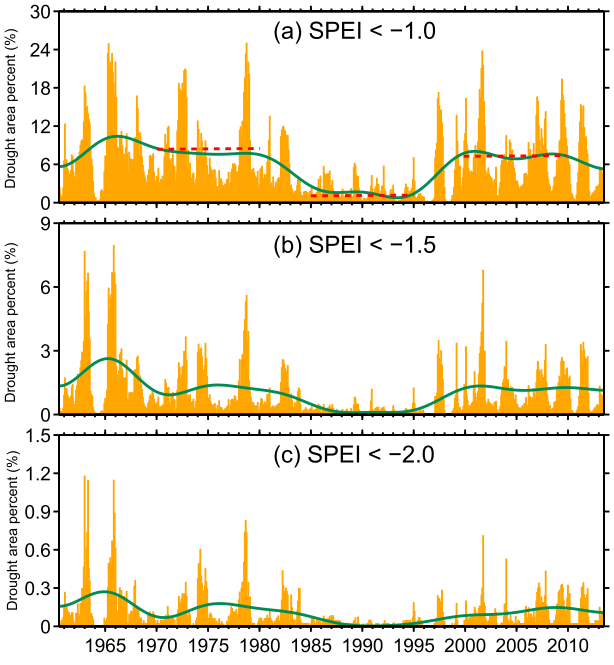

FIG. 4. Temporal variations in the monthly area coverage (in %) for (a) moderate, (b) severe, and (c) extreme drought conditions in China. The drought areas are calculated based on the 12-month SPEI_PM. The time periods denoted by the dashed lines are discussed in this study.

at sparse stations in NWC have continued to decrease in recent years. Relatively small changes are found for the stations over eastern China; however, significant decadal changes are observed in this region, with more drought events occurring during the periods 1970–80 and 2000–10 and less occurring during the period 1985–95. Additionally, the annual cycles of the droughts in China also vary from decades and regions. In 2000–10, droughts over NEC and NM mainly occur in boreal autumn and droughts over NWC prevail in spring and summer. Over most regions of eastern China, including NC, HH, and JN, droughts mainly happen in spring and early summer (figure not shown).

The decadal changes in drought frequency in the arid, semiarid, semihumid, and humid regions (Fig. 7) reveal that the minimum drought frequency occurred during the period 1985–95 in these four regions and for all of China. In the arid region, droughts were more common during the period 1970–80, with relatively few incidents in recent years. In the semiarid and semihumid regions, droughts occurred with similar frequencies during the periods 1970–80 and 2000–10, with a much higher frequency of occurrence compared with the period 1985–95. However, the changes in the humid region are different. The drought frequencies during the periods 1985–95 and 1970–80 are comparable, with less drought events occurring in this region. However, a relatively high drought frequency is found for the period 2000–10 in the humid region, which indicates that the dry conditions over most of China have been enhanced during the most recent decade, especially in the humid region.

In addition to changes in drought frequency, variations in drought intensity were also investigated over China. Figure 8 illustrates the spatial distributions of the decadal changes in drought intensity (mean values of the SPEI < -1.0) over the past several decades. Clearly, the spatial patterns of changes in drought intensity are similar to those of drought frequency. The regions with decreases in drought frequency are generally accompanied with a reduction in drought intensity (and vice versa). During the period 1985–95, the drought intensity was much weaker over most of China compared to the period 1970–80. However, the intensity increases during

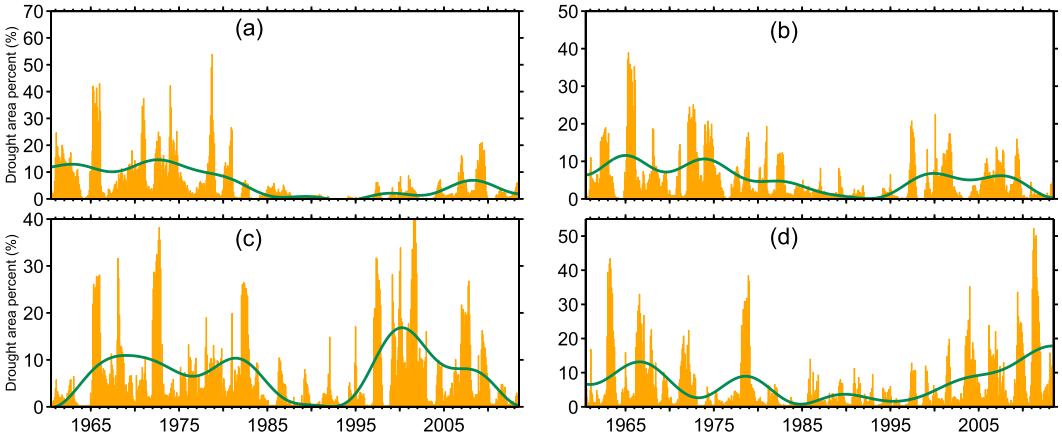

FIG. 5. Temporal variations in the monthly area (in %) of drought conditions in which the 12-month SPEI_PM < -1.0 in China during the period 1961–2012. (a) The arid region, (b) the semiarid region, (c) the semihumid region, and (d) the humid region are shown.

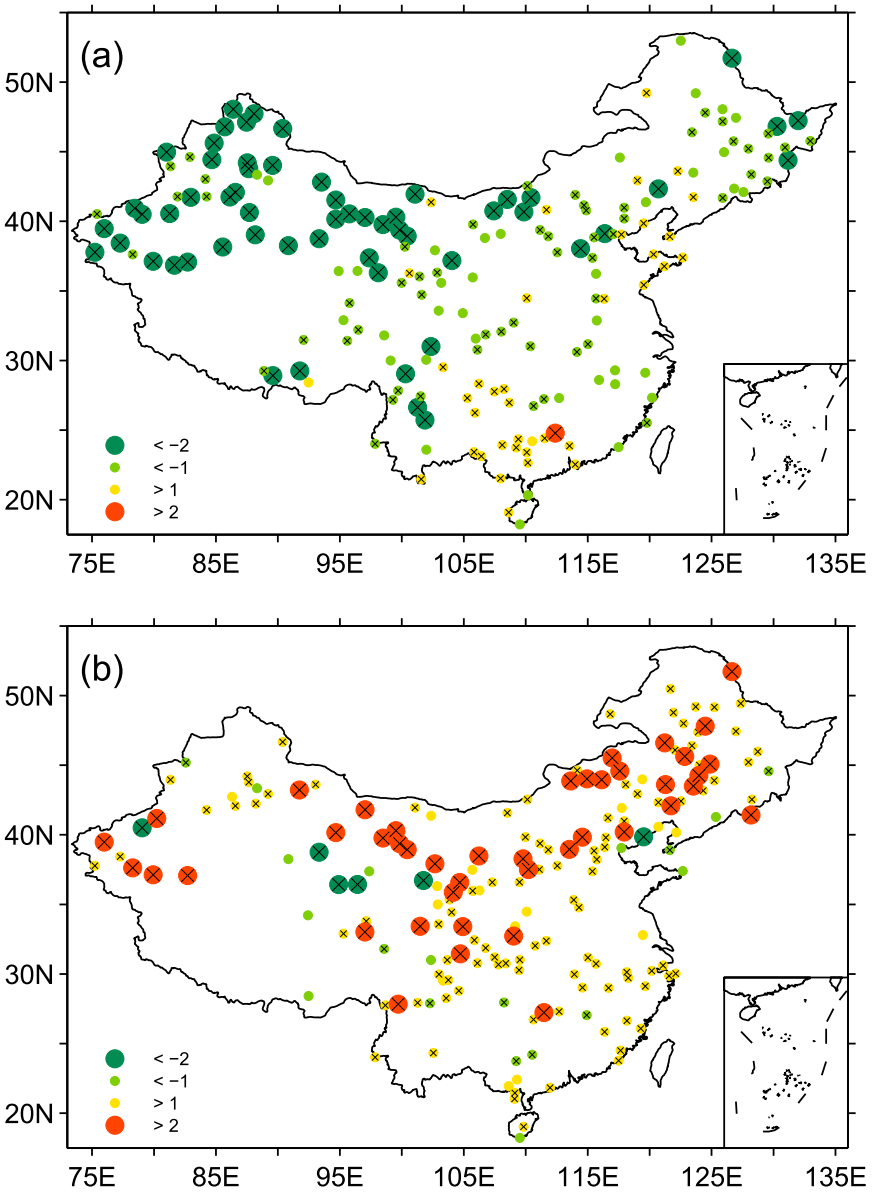

FIG. 6. Spatial distributions of the decadal variations in drought frequency (3-month SPEI_PM < -1.0) over China during recent decades. (a) The drought frequency difference between the period from 1985 to 1995 and the period from 1970 to 1980, (b) difference between the period from 2000 to 2010 and the period from 1985 to 1995. The crosses indicate that the differences are significant at the 95% confidence level using a Student's *t* test.

the period 2000–10 in most regions of China, particularly at stations in NEC, NC, HH, NM, and NWC. This result further demonstrates that the dry conditions in China have been enhanced in recent years, especially in northern China. This result is further validated by the temporal variations in drought intensity (Fig. 9). Two drought intensity peaks have occurred during the past 50 yr for each subregion and for all of China. The results indicate that the droughts in China were relatively severe during the 1960s, 1970s, and 2000s and relatively weak during the 1980s and 1990s. Similar characteristics can be seen for the four subregions, particularly for the arid region, which has exhibited a relatively large change in drought intensity during recent decades.

Based on the spatial distribution of drought duration for China during the period 1961–2012, which is defined as the longest number of consecutive months in which the 3-month SPEI < -1.0, some portions of NWC, NEC, NC, NM, and SWC experienced droughts exceeding 12 months in duration, with some even

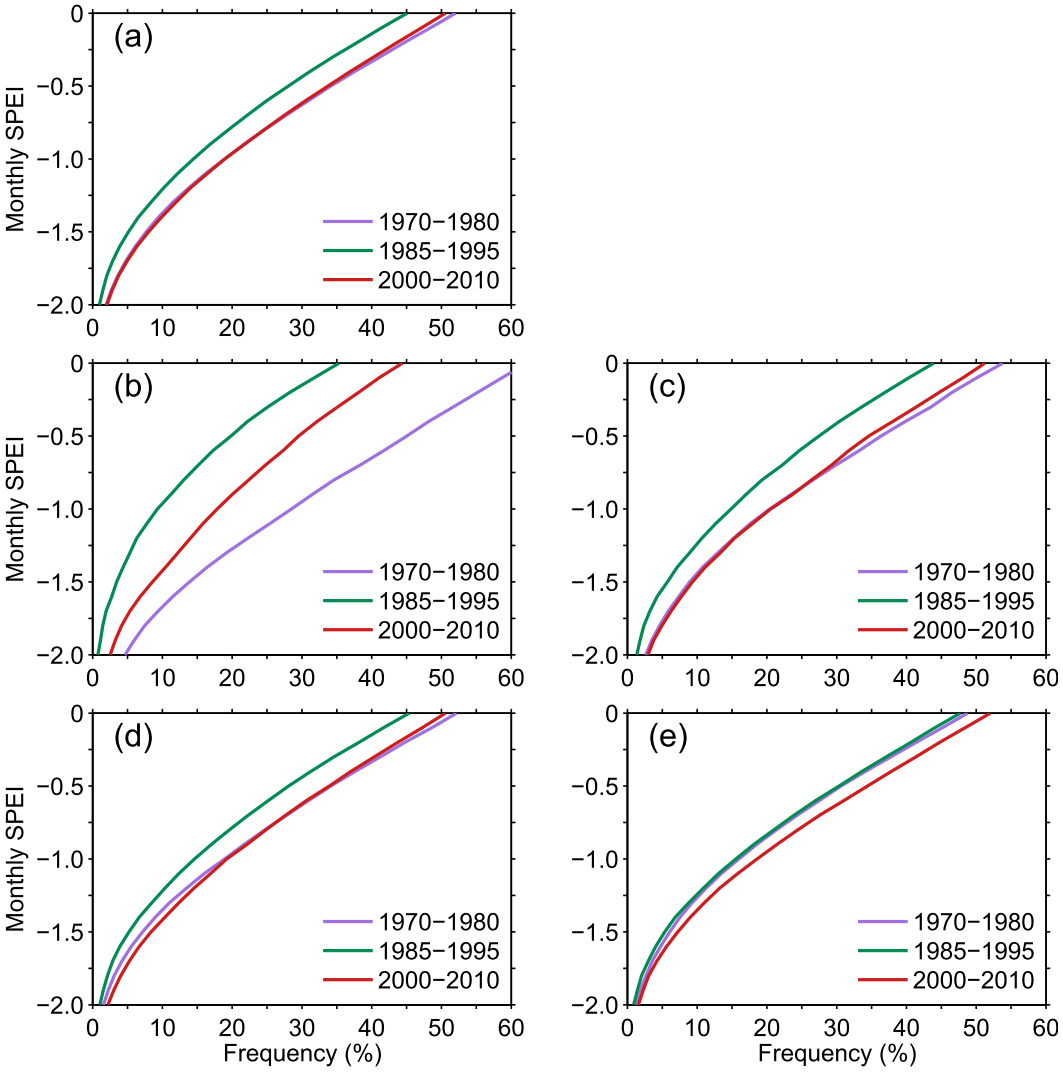

FIG. 7. Drought frequency distributions for different regions in China. (a) China, (b) the arid region, (c) the semiarid region, (d) the semihumid region, and (e) the humid region are shown.

exceeding 18 months at stations in Xinjiang Province. According to the available data, the most severe droughts in 2009/10 and 2011/12 across SWC (including Yunnan, Sichuan, Guizhou, Guangxi, and Chongqing Provinces) exhibited the longest duration compared with other drought events during recent decades. Consecutive drought events generally cause relatively large effects on agriculture, ecosystems, and society. Thus, the decadal variations in the frequency and intensity of consecutive drought events, which are defined based on events in which the SPEI_PM < -1.0 (using a 3-month scale) for at least 6 months, are presented in Fig. 10. A reduction in the number of consecutive drought events is found over China for the period 1985–95 when compared with the period 1970–80; some stations exhibit decreases exceeding two events, especially in NWC. However, during the period 2000–10, this decrease ended and was followed by an increase in the occurrence of consecutive drought events at most stations across China. Based on the analysis of intensity changes, a significant increase in the intensity of the consecutive drought events has occurred in recent years. Furthermore, for some stations across China, no consecutive drought events occurred in the early period (1985–95), while such events occurred, sometimes exceeding two events, during the period 2000–10. These results demonstrate that the dry conditions have been enhanced in recent years across most of China; this drying trend will intensify with continued warming in the future.

The aforementioned analyses reveal that droughts in China have featured a significant interdecadal variation over the past 50 yr and that these events have become

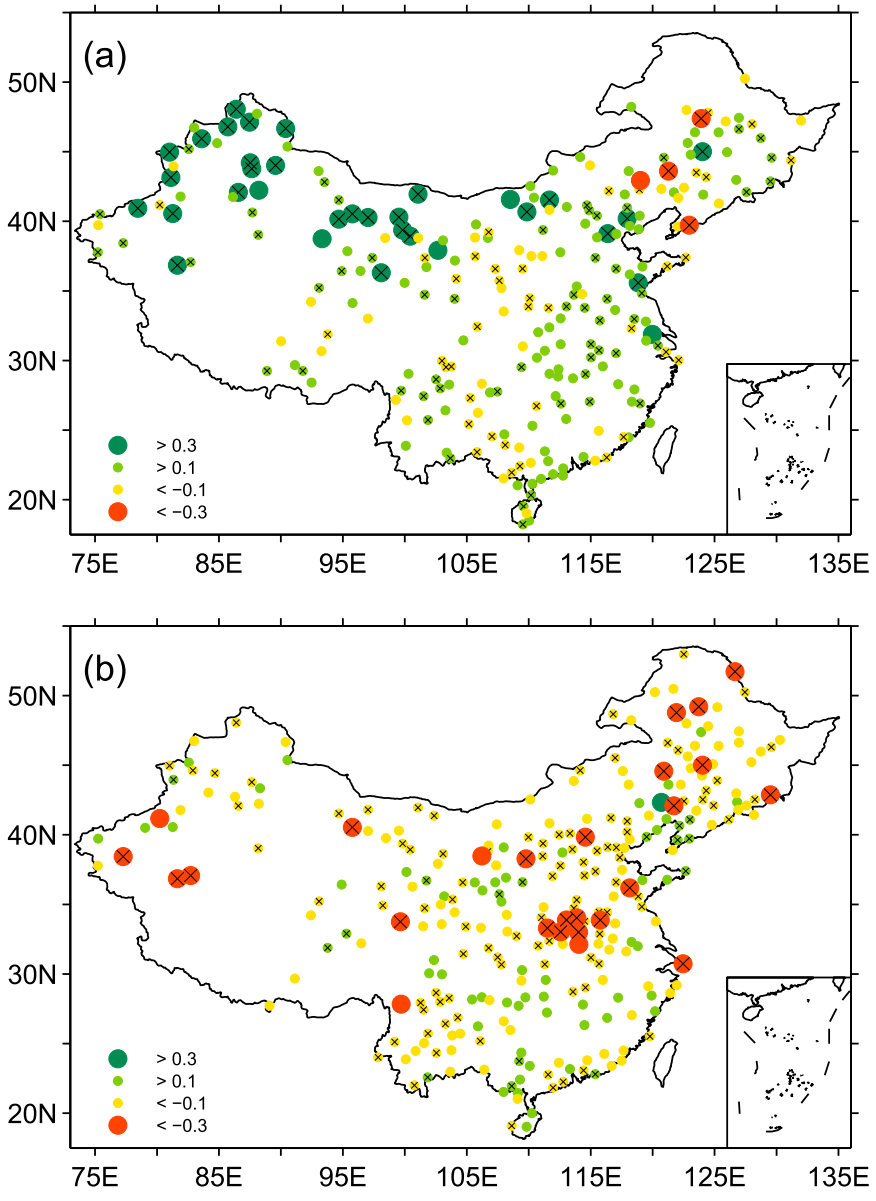

FIG. 8. As in Fig. 6, but for drought intensity changes.

more frequent and severe in most regions of China in recent years. Correspondingly, the associated dry conditions have been enhanced. These results are very important and valuable to both the public and government; more attention to this topic is needed.

5. Responses to precipitation and temperature changes

The SPEI_PM measures the accumulated effect of a deficit/surplus in the water balance between the actual monthly precipitation and the required precipitation. The required precipitation is generally a function of air temperature. Thus, variations in the SPEI_PM primarily include effects from precipitation and air temperature anomalies. Several studies have revealed the influences of temperature and precipitation anomalies on the PDSI and other related indices (e.g., Guttman 1991; Hu and Willson 2000). For example, previous results have indicated that precipitation anomalies tend to dominate changes in the PDSI during the cold season due to the inherent evaporation minimum during this season, while the ambient temperature becomes important for the PDSI in the warm season. However, such analysis has

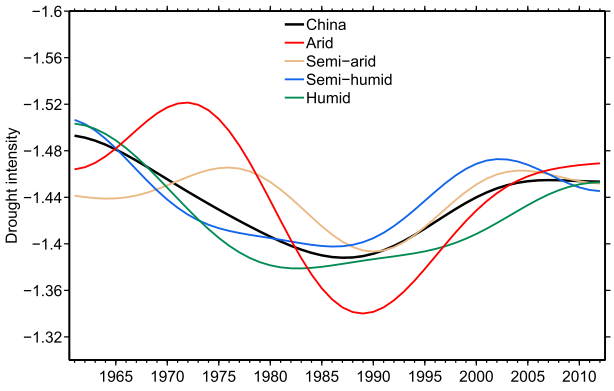

FIG. 9. Decadal variations in drought intensity for different regions in China. A 21-yr low-pass filtering process was used for each series.

not been applied to the SPEI_PM. Moreover, the precipitation and temperature effects on the SPEI_PM have not been thoroughly investigated thus far.

Several experiments are used to illustrate the effects of precipitation and temperature, including scenario 1, in which the temperature is assumed to increase progressively by 2°C, while the actual precipitation variability for each month is based on observations from 1961 to 2012; scenario 2, in which the precipitation is increased progressively by 10%, while the actual temperatures are used; and scenario 3, in which the temperature increases progressively by 2°C in conjunction with a continuous increase in precipitation of 10%. The SPEI_PM is recalculated after adding these perturbations to the monthly temperature and precipitation data, respectively. Additionally, the SPEI_PM is also calculated using the historical data to provide a basis for comparison and to identify the responses of the SPEI_PM to temperature and precipitation changes.

Figure 11 shows the spatial patterns for the relative changes in drought frequency and intensity for the three perturbation scenarios relative to the real climate conditions. In scenario 1, which experiences a progressive temperature increase of 2°C, droughts increase significantly across China over the last two decades, with a relatively large increase in northern China and a smaller increase in southern China. The average drought frequency in China increases by 19%; however, the increase varies regionally. The largest increase occurs in the arid region (by 53%), which is followed by the semiarid and semihumid regions (by 20%) and the humid region (by 9%). Additionally, for the case in which the temperature progressively increases by 2°C, the drought severity is reinforced due to the high water demand of potential evapotranspiration (PET) (based on the SPEI_PM), with drought intensity increasing across China. The average drought intensity in China increases by 13%. The changes in drought severity are similar to those of drought frequency, with a relatively large increase in drought severity in the arid region (by 31%), which is followed by the semiarid and semihumid regions (14%) and the humid region (7%). This finding suggests that if precipitation remains constant, the ambient temperature will play a major role in determining future drought severity in China, which is consistent with the results of previous studies (e.g., Vicente-Serrano et al. 2010; Chen and Sun 2015).

If the precipitation is increased progressively by 10% (scenario 2), the drought response is opposite that of increasing the air temperature, that is, droughts are mitigated across China. However, a relatively large response in the SPEI_PM to increased precipitation is found in southern China, while a relatively small response occurs in the other regions. The same result is also applied to drought severity across China. This conclusion may be partially associated with the relatively large increase in precipitation (i.e., 10%) in southern China, leading to relatively large precipitation variability compared with the other regions. Considering China as a whole, drought frequency decreases by 11%, and the corresponding drought intensity decreases by 9% if the precipitation increases by 10%. For the arid region, relatively small responses are found at most stations, except for several stations in northern Xinjiang Province. The average frequency and intensity in this region decrease by 4% and 3%, respectively. The responses in the semiarid and semihumid regions are much larger; that is, the frequency and intensity decrease by 9% and 8%, respectively. The most noticeable changes occur in the humid region, in which the frequency and intensity of droughts decrease by 14% and 11%, respectively.

Based on the aforementioned analyses of scenarios 1 and 2, a spatial inhomogeneity is present in the response of the SPEI_PM to temperature and precipitation perturbations; this response varies regionally because of local variations in total precipitation amounts. In the humid region, there is enough precipitation to meet the high water demand of PET; this is true even if the air temperature is assumed to increase significantly. Thus, the responses in this region are relatively large for precipitation changes compared with temperature changes. However, this result is reversed in the other regions in China, especially in the arid and semiarid regions. This difference is because there is not enough precipitation to meet the water demand of PET, which is true even if the local precipitation is assumed to increase significantly. Thus, droughts in these regions exhibit greater sensitivity to temperature changes than to precipitation changes. To further illustrate this point, another experiment is performed, namely, scenario 3. In this scenario,

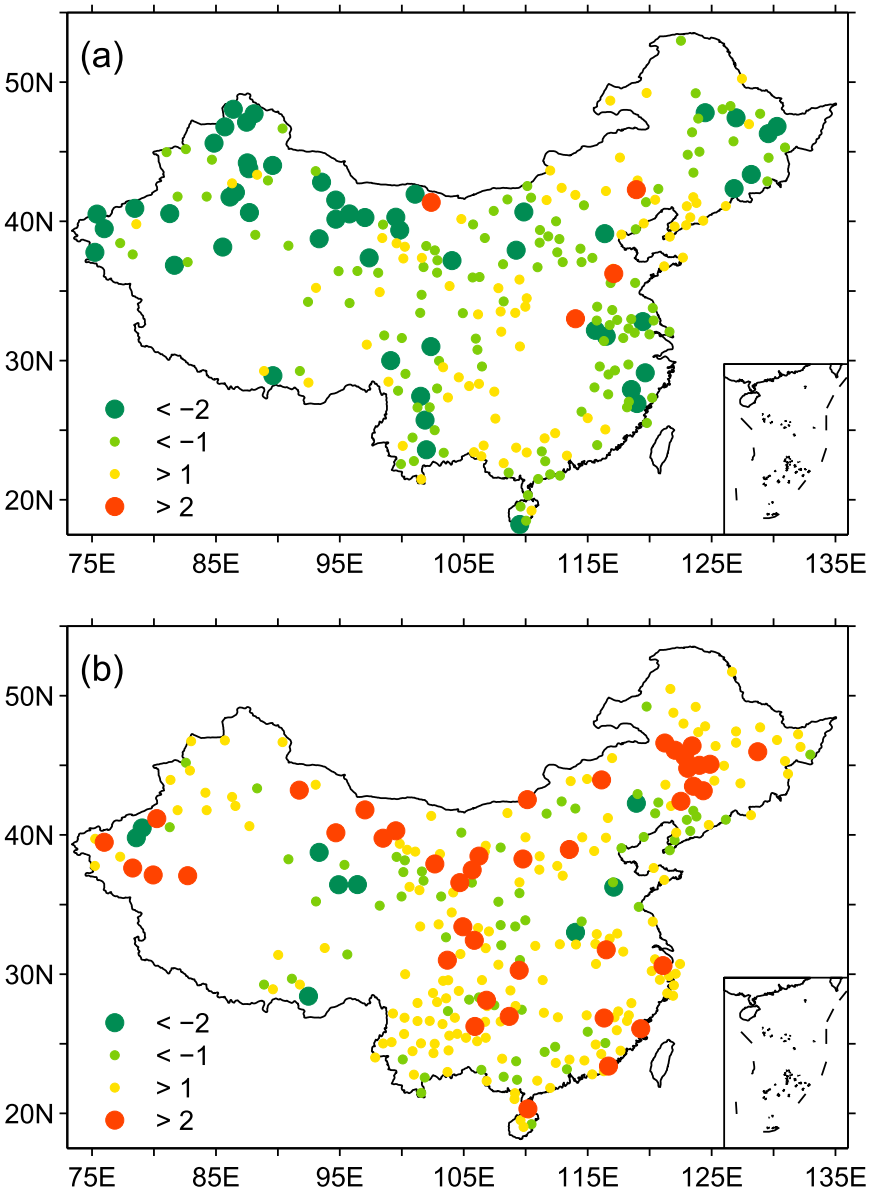

FIG. 10. Decadal variations in the frequency of consecutive drought events (defined as those events in which the 3-month SPEI_PM < -1.0 for at least 6 months). (a) Differences between the period from 1985 to 1995 and the period from 1970 to 1980. (b) Differences between the period from 2000 to 2010 and the period from 1985 to 1995.

drought frequency decreases substantially in the humid region (by 6%) and increases in the other regions (by 47% in the arid region and by 10% in the semiarid and semihumid regions). Similar changes are found for drought intensity, that is, a decrease of 5% in the humid region and an increase of 27% in the arid region and 7% in the semiarid and semihumid regions.

Based on the above analyses, the SPEI_PM exhibits different responses to temperature and precipitation anomalies that vary regionally across China. Relatively large responses in droughts to temperature perturbations occur primarily over northern China, while large responses to precipitation anomalies are found over southern China. These results may be associated with the assumed extent of the temperature and precipitation changes. Therefore, experiments in which the temperature is increased by 4°C and the precipitation is increased by 20% are also explored; the results are similar to those of aforementioned scenarios except that the response is stronger, that is, approximately doubled.

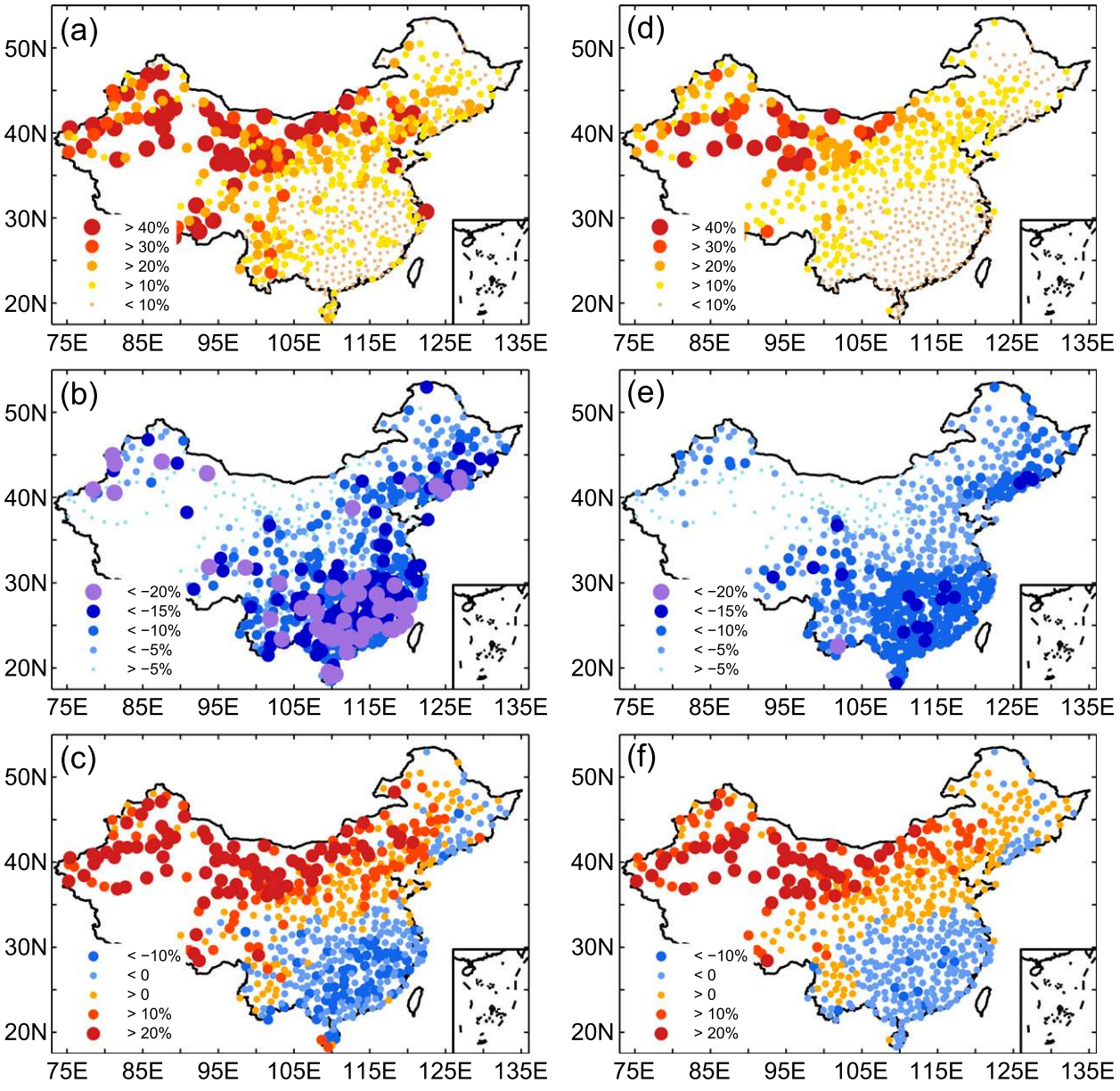

FIG. 11. Spatial patterns in the responses of drought (3-month SPEI_PM < -1.0) (left) frequency and (right) intensity to temperature and precipitation changes. The responses of drought (a) frequency and (d) intensity to temperature changes (progressive increase of 2°C) when actual precipitation variability is used for each month between 1961 and 2012. (b),(e) The results for increased precipitation (by 10%). (c),(f) The results in which both the precipitation and temperature are perturbed over the same period. The response is defined as the relative change compared to the results based on the original SPEI_PM during the period 1993–2012.

However, another important question is raised: what are the actual roles of temperature and precipitation variations in drought changes over China during recent decades? This is a complicated question to answer because of the nonlinear interactions among temperature, precipitation, and drought. Here, we attempt to address this question via sensitivity experiments by assuming a linear relationship among the effects of several factors (e.g., precipitation, temperature, and wind) on droughts in China. The experiments are designed as follows: Experiment 1 assumes that the air temperatures remain constant based on the values in 1960 for each month; no changes are applied to the other factors. Experiment 2 applies the same assumption to precipitation variations. The SPEI_PM is recalculated on the basis of these datasets. The approximate roles of temperature and

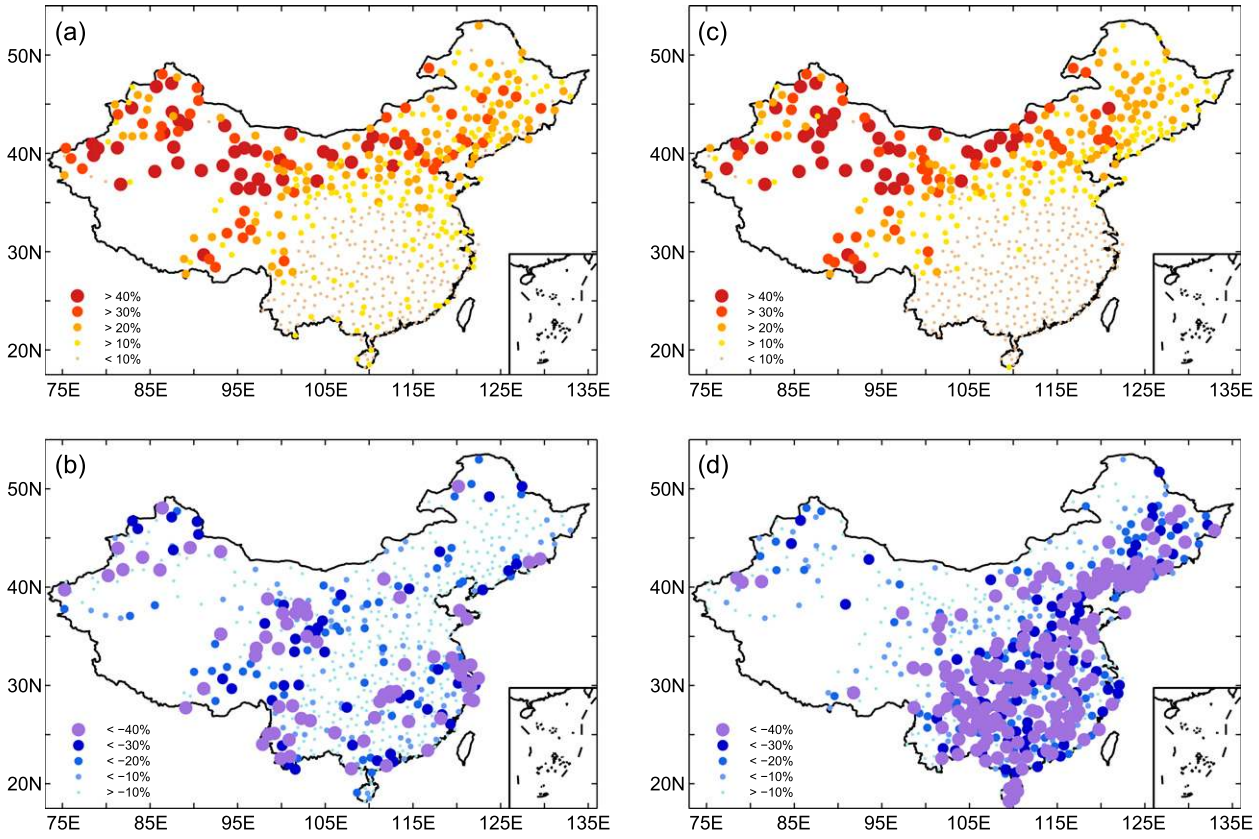

FIG. 12. Responses of drought to real temperature and precipitation changes during recent decades. (a),(c) The relative changes in drought frequency and intensity due to real temperature changes. (b),(d) The results due to real precipitation changes. Here, the response is defined as the relative difference between the real climate conditions and the experiments in which the temperature and precipitation are assumed to remain constant for the entire analysis period based on the values for each month in 1960.

precipitation anomalies on droughts can be estimated from the difference between the real climate conditions and these two experiments. The corresponding results for the changes in drought frequency and intensity due to temperature and precipitation variations during the last two decades are shown in Fig. 12. The temperature variations over recent decades exhibit relatively large positive effects on the occurrence of drought over northern China, including Tibet, while relatively small effects are found over southern China. The results indicate that approximately 42% of the observed droughts have been caused by temperature anomalies over the last two decades in the arid region; this proportion decreases to approximately 22% for the semiarid and semihumid regions and only 5% for the humid region. Similar magnitudes are found for the effects on drought severity, that is, approximately 45% in the arid region, 22% in the semiarid and semihumid regions, and 5% in the humid region. This spatial inhomogeneity of the temperature effects may be interpreted via two causes. One cause is the spatial inhomogeneity of the total precipitation amount in China (as discussed above in this section). The other cause is the spatial inhomogeneity of the temperature increase during recent decades, with a relatively large increase over northern China and Tibet and a small increase over southern China. The results are different when considering precipitation variations during recent decades. Droughts are found to decrease in China due to the precipitation variations, especially over some parts of southern China, north Xinjiang, and Tibet. Moreover, the drought severity decreases over southern China and some parts of north and northeast China because droughts are primarily modulated by precipitation variations in these regions (the precipitation amounts are sufficient to meet the water demand of PET). The drought severity is mitigated by approximately 35% in the humid region compared to the experiment in which precipitation remains constant, approximately 21% in the semiarid and semihumid regions, and 9% in the arid region. Additionally, the drought occurrences decrease by approximately 10%, 7%, and 5% in the arid region, semiarid and

semihumid regions, and humid region, respectively, due to the effects of precipitation variations in recent decades.

6. Conclusions and discussion

There are vast differences in the annual accumulated potential evapotranspiration between Thornthwaite (1948) parameterization and the FAO-endorsed Penman–Monteith parameterization (Allen et al. 1998) estimates. Although some studies (e.g., Beguería et al. 2014) have documented that these methods produce similar estimates of the SPEI from the global perspective, several pronounced differences are found when focusing solely on China, especially in its arid regions. The effects of temperature changes on drought characteristics are generally amplified in the arid region of China when ET is calculated according to the Thornthwaite approach. However, the results from the SPEI_PM, in which ET is calculated using the more realistic PM equation, are more reasonable and better reflect climate change conditions in this region. Nevertheless, the site-observed soil moisture and streamflow variations are also used in this study for additional comparisons with regard to the performance of the SPEI_TH and the SPEI_PM. Because the SPEI_PM is more robust than the SPEI_TH, the SPEI_PM is recommended for investigating changes in drought characteristics over China based on updated data covering the period 1961–2012.

Changes in several drought characteristics are investigated based on data for the past 50 yr, including drought frequency, intensity, and percentage of area affected. The results indicate that droughts over China exhibit a well-defined decadal variation during the past 50 yr, with more frequent droughts occurring before the 1980s and in the 2000s and fewer droughts in the 1980s and 1990s. Based on changes in drought area, several regional differences are detected. The drought area is found to have increased since the late 1990s in the arid and semiarid regions; the increase was much smaller than in the 1960s and 1970s. Moreover, the increases in the semihumid and humid regions are found to be more substantial, especially in the humid region, which is where several extensive droughts have recently occurred. The analysis also reveals that droughts in China have become more frequent and severe in the recent decade, which is concomitant with a significant increase in consecutive drought events. This finding suggests that the dry conditions across China have been enhanced in recent years, particularly for some stations in northern China that have experienced relatively large increase in both drought frequency and severity.

Further analyses illustrate that temperature and precipitation changes exhibit different roles in determining droughts in China; these different roles are primarily related to the extent of the changes and different climate variability. When temperature and precipitation perturbations are added to the data, respectively, different drought responses are observed. The responses in the SPEI_PM to temperature and precipitation anomalies vary regionally across China. Relatively large responses to temperature changes are found over northern China, especially in the arid region, while relatively small responses occur in southern China, especially in the humid region. The opposite shifts are found in response to precipitation perturbations, with relatively large responses in southern China and small response in northern China. This spatial inhomogeneity in the responses is partially associated with the local variations in total precipitation amounts. These results are also true for the real climate conditions. The actual temperature anomalies during recent decades exhibit larger contributions to the occurrences of drought over northern China, while a smaller contribution is found over southern China. Temperature contributions are found to cause approximately 42%, 22%, and 5% of droughts in the arid region, the semiarid and semihumid regions, and the humid region, respectively. The actual precipitation anomalies exhibit relatively large effects on drought severity compared with drought occurrences, with a large contribution in the humid region (35%), which is followed by the semiarid and semihumid regions (21%) and the arid region (9%). Based on these experiment analyses, we can conclude that the rapid warming of China in recent decades presents a relatively greater role in determining droughts than that of precipitation variations. However, more validations are still needed.

Changes in drought characteristics during the past 50 yr in China are detected and analyzed in this study; however, the mechanism for these changes remains unknown due to the complexity of drought occurrences (Dai 2011a). Thus far, some studies have shown that wet–dry variations in northern China are statistically related to the phase transition of the Pacific decadal oscillation (PDO) (e.g., Ma 2007); however, it is uncertain if this change is related to natural variability or anthropogenic changes. Additionally, the droughts in the humid region (especially in SWC) have increased substantially and have become much more severe in recent years. A possible mechanism for the specified drought events that have recently occurred has been well addressed in this region, particularly in SWC (e.g., Yang et al. 2012). However, a mechanism for explaining the recent drying trend remains unknown. More studies are needed to address these issues in the future and to improve our understanding of drought changes in China.

Acknowledgments. We sincerely acknowledge the anonymous reviewers whose kind and valuable comments greatly improved the manuscript. This research was jointly supported by the ''Strategic Priority Research Program-Climate Change: Carbon Budget and Relevant Issues'' of the Chinese Academy of Sciences (XDA05090306), the National Natural Science Foundation of China (41305061), the National Basic Research Program of China (2012CB955401), and the National Natural Science Foundation of China (41421004).

REFERENCES

Allen, R. G., L. S. Pereira, D. Raes, and M. Smith, 1998: Crop evapotranspiration: Guidelines for computing crop water requirements. FAO Irrigation and Drainage Paper 56, 300 pp.

Beguería, S., S. M. Vicente-Serrano, F. Reig, and B. Latorre, 2014: Standardized precipitation evapotranspiration index (SPEI) revisited: Parameter fitting, evapotranspiration models, tools, datasets and drought monitoring. *Int. J. Climatol.,* **34,** 3001–3023, doi:10.1002/joc.3887.

Chen, H. P., and J. Q. Sun, 2015: Drought response to air temperature change over China on the centennial scale. *Atmos. Oceanic Sci. Lett.,* **8,** 113–119, doi:10.3878/AOSL20140089.

——, ——, and H. J. Wang, 2012a: A statistical downscaling model for forecasting summer rainfall in China from DEMETER hindcast datasets. *Wea. Forecasting,* **27,** 608–628, doi:10.1175/WAF-D-11-00079.1.

——, ——, and K. Fan, 2012b: Possible mechanism for the interdecadal change of Xinjiang summer precipitation. *Chin. J. Geophys.,* **55,** 267–274, doi:10.1002/cjg2.1721.

——, ——, and X. L. Chen, 2013: Future changes of drought and flood events in China under a global warming scenario. *Atmos. Oceanic Sci. Lett.,* **6,** 8–13.

Cong, Z., D. Yang, B. Gao, H. Yang, and H. Hu, 2009: Hydrological trend analysis in the Yellow River basin using a distributed hydrological model. *Water Resour. Res.,* **45,** W00A13, doi:10.1029/2008WR006852.

Dai, A. G., 2011a: Drought under global warming: A review. *Wiley Interdiscip. Rev.: Climate Change,* **2,** 45–65, doi:10.1002/wcc.81.

——, 2011b: Characteristics and trends in various forms of the Palmer drought severity index during 1900–2008. *J. Geophys. Res.,* **116,** D12115, doi:10.1029/2010JD015541.

——, 2012: Increasing drought under global warming in observations and models. *Nat. Climate Change,* **3,** 52–58, doi:10.1038/nclimate1633.

——, K. E. Trenberth, and T. Qian, 2004: A global dataset of Palmer drought severity index for 1870–2002: Relationship with soil moisture and effects of surface warming. *J. Hydrometeor.,* **5,** 1117–1130, doi:10.1175/JHM-386.1.

Duan, H., S. Wang, and J. Feng, 2013: The drought in China in summer 2013 and its impact and cause (in Chinese). *J. Arid Meteor.,* **31,** 633–640.

Dubrovsky, M., M. D. Svoboda, M. Trnka, M. J. Hayes, D. A. Wilhite, Z. Zalud, and P. Hlavinka, 2009: Application of relative drought indices in assessing climate-change impacts on drought conditions in Czechia. *Theor. Appl. Climatol.,* **96,** 155–171, doi:10.1007/s00704-008-0020-x.

Field, C. B., and Coauthors, 2012: *Managing the Risks of Extreme Events and Disasters to Advance Climate Change Adaptation.* Cambridge University Press, 582 pp.

Gao, H., and S. Yang, 2009: A severe drought event in northern China in winter 2008–2009 and the possible influences of La Niña and Tibetan Plateau. *J. Geophys. Res.,* **114,** D24104, doi:10.1029/2009JD012430.

Guttman, N. B., 1991: A sensitivity analysis of the Palmer hydrologic drought index. *J. Amer. Water Resour. Assoc.,* **27,** 797–807, doi:10.1111/j.1752-1688.1991.tb01478.x.

——, 1998: Comparing the Palmer drought severity index and the standardized precipitation index. *J. Amer. Water Resour. Assoc.,* **34,** 113–121, doi:10.1111/j.1752-1688.1998.tb05964.x.

Hu, Q., and G. D. Willson, 2000: Effects of temperature anomalies on the Palmer drought severity index in the central United States. *Int. J. Climatol.,* **20,** 1899–1911, doi:10.1002/1097-0088(200012)20:15<1899::AID-JOC588>3.0.CO;2-M.

Huang, R. H., Y. Liu, L. Wang, and L. Wang, 2012: Analyses of the causes of severe drought occurring in southwest China from the fall of 2009 to the spring of 2010 (in Chinese). *Chin. J. Atmos. Sci.,* **36,** 443–457.

Jensen, M. E., R. D. Burman, and R. G. Allen, 1990: Evapotranspiration and irrigation water requirements. ASCE Manual of Practice 70, 360 pp.

Liu, K., and D. B. Jiang, 2014: Interdecadal change and cause analysis of extreme summer and winter droughts over China (in Chinese). *Chin. J. Atmos. Sci.,* **38,** 309–321.

Lu, E., Y. Luo, R. Zhang, Q. Wu, and L. Liu, 2011: Regional atmospheric anomalies responsible for the 2009–2010 severe drought in China. *J. Geophys. Res.,* **116,** D2114, doi:10.1029/2011JD015706.

Ma, Z. G., 2007: The interdecadal trend and shift of dry/wet over the central part of north China and their relationship to the Pacific decadal oscillation (PDO). *Chin. Sci. Bull.,* **52,** 2130–2139, doi:10.1007/s11434-007-0284-z.

——, and C. B. Fu, 2001: Trend of surface humid index in the arid area of northern China (in Chinese). *Acta Meteor. Sin.,* **59,** 773–746.

——, and ——, 2006: Some evidence of drying trend over northern China from 1951 to 2004. *Chin. Sci. Bull.,* **51,** 2913–2925, doi:10.1007/s11434-006-2159-0.

McKee, T. B., N. J. Doesken, and J. Kleist, 1993: The relationship of drought frequency and duration to time scales. Preprints, *Eighth Conf. on Applied Climatology,* Anaheim, CA, Amer. Meteor. Soc., 179–184.

Orlowsky, B., and S. I. Seneviratne, 2013: Elusive drought: Uncertainty in observed trends and short- and long-term CMIP5 projections. *Hydrol. Earth Syst. Sci.,* **17,** 1765–1781, doi:10.5194/hess-17-1765-2013.

Palmer, W. C., 1965: Meteorological drought. U.S. Weather Bureau Research Paper 45, 58 pp.

Roderick, M. L., L. D. Rotstayn, G. D. Farquhar, and M. T. Hobbins, 2007: On the attribution of changing pan evaporation. *Geophys. Res. Lett.,* **34,** L17403, doi:10.1029/2007GL031166.

Sen, P. K., 1968: Estimates of the regression coefficient based on Kendall's tau. *J. Amer. Stat. Assoc.,* **63,** 1379–1389, doi:10.1080/01621459.1968.10480934.

Sentelhas, P. C., T. J. Gillespie, and E. A. Santos, 2010: Evaluation of FAO Penman–Monteith and alternative methods for estimating reference evapotranspiration with missing data in southern Ontario, Canada. *Agric. Water Manage.,* **97,** 635–644, doi:10.1016/j.agwat.2009.12.001.

Sheffield, J., E. F. Wood, and M. L. Roderick, 2012: Little change in global drought over the past 60 years. *Nature,* **491,** 435–438, doi:10.1038/nature11575.

Si, D., Y. H. Ding, and Y. J. Liu, 2009: Decadal northward shift of the meiyu belt and the possible cause. *Chin. Sci. Bull.,* **54,** 4742–4748, doi:10.1007/s11434-009-0385-y.

Song, L., Z. Deng, and A. Dong, 2003: *Hot Topics of Global Change—Drought* (in Chinese). China Meteorological Press, 162 pp.

Spinoni, J., G. Naumann, H. Carrao, P. Barbosa, and J. Vogt, 2014: World drought frequency, duration, and severity for 1951–2010. *Int. J. Climatol.,* **34,** 2792–2804, doi:10.1002/joc.3875.

Stocker, T. F., and Coauthors, 2013: *Climate Change 2013: The Physical Science Basis.* Cambridge University Press, 1535 pp.

Sun, J. Q., 2014: Record-breaking SST over mid-North Atlantic and extreme high temperature over the Jianghuai–Jiangnan region of China in 2013. *Chin. Sci. Bull.,* **59,** 3465–3470, doi:10.1007/s11434-014-0425-0.

Thornthwaite, C. W., 1948: An approach toward a rational classification of climate. *Geogr. Rev.,* **38,** 55–94, doi:10.2307/210739.

Trenberth, K. E., A. G. Dai, G. van der Schrier, P. D. Jones, J. Barichivich, K. R. Briffa, and J. Sheffield, 2014: Global warming and changes in drought. *Nat. Climate Change,* **4,** 17–22, doi:10.1038/nclimate2067.

van der Schrier, G., P. D. Jones, and K. R. Briffa, 2011: The sensitivity of the PDSI to the Thornthwaite and Penman-Monteith parameterizations for potential evapotranspiration. *J. Geophys. Res.,* **116,** D03106, doi:10.1029/2010JD015001.

Vicente-Serrano, S. M., S. Beguería, and J. I. López-Moreno, 2010: A multiscalar drought index sensitive to global warming: The standardized precipitation evapotranspiration index. *J. Climate,* **23,** 1696–1718, doi:10.1175/2009JCLI2909.1.

Wang, A., D. Lettenmaier, and J. Sheffield, 2011: Soil moisture drought in China, 1950–2006. *J. Climate,* **24,** 3257–3271, doi:10.1175/2011JCLI3733.1.

Wang, H. J., and Coauthors, 2012: Extreme climate in China: Facts, simulation and projection. *Meteor. Z.,* **21,** 279–304, doi:10.1127/0941-2948/2012/0330.

Wang, L., W. Chen, and W. Zhou, 2014: Assessment of future drought in southwest China based on CMIP5 multimodel projections. *Adv. Atmos. Sci.,* **31,** 1035–1050, doi:10.1007/s00376-014-3223-3.

Wells, N., S. Goddard, and M. J. Hayes, 2004: A self-calibrating Palmer drought severity index. *J. Climate,* **17,** 2335–2351, doi:10.1175/1520-0442(2004)017<2335:ASPDSI>2.0.CO;2.

Xin, X., R. Yu, T. Zhou, and B. Wang, 2006: Drought in late spring of south China in recent decades. *J. Climate,* **19,** 3197–3206, doi:10.1175/JCLI3794.1.

Yan, Z. W., J. J. Xia, C. Qian, and W. Zhou, 2011: Changes in seasonal cycle and extremes in China during the period 1960–2008. *Adv. Atmos. Sci.,* **28,** 269–283, doi:10.1007/s00376-010-0006-3.

Yang, J., D. Gong, W. Wang, M. Hu, and R. Mao, 2012: Extreme drought event of 2009/2010 over southwestern China. *Meteor. Atmos. Phys.,* **115,** 173–184, doi:10.1007/s00703-011-0172-6.

Yu, M. X., Q. F. Li, G. Lu, T. Cai, W. Xie, and X. Bai, 2013: Investigation into the impacts of the Gezhouba and the Three Gorges reservoirs on the flow regime of the Yangtze River. *J. Hydrol. Eng.,* **18,** 1098–1106, doi:10.1061/(ASCE)HE.1943-5584.0000545.

——, ——, M. J. Hayes, M. D. Svoboda, and R. Heim, 2014: Are droughts becoming more frequent or severe in China based on the standardized precipitation evapotranspiration index: 1951–2010? *Int. J. Climatol.,* **34,** 545–558, doi:10.1002/joc.3701.

Zheng, J. Y., J. Bian, Q. Ge, Z. Hao, Y. Yin, and Y. Liao, 2013: The climate regionalization in China for 1981–2010 (in Chinese). *Chin. Sci. Bull.,* **58,** 3088–3099.

Zhu, Y. L., H. J. Wang, W. Zhou, and J. H. Ma, 2011: Recent changes in the summer precipitation pattern in east China and the background circulation. *Climate Dyn.,* **36,** 1463–1473, doi:10.1007/s00382-010-0852-9.

Zou, X., P. Zhai, and Q. Zhang, 2005: Variations in droughts over China: 1951–2003. *Geophys. Res. Lett.,* **32,** L04707, doi:10.1029/2004GL021853.